frontiers

Supplementary Material

SUPPLEMENTARY INFORMATION

S1 MODEL

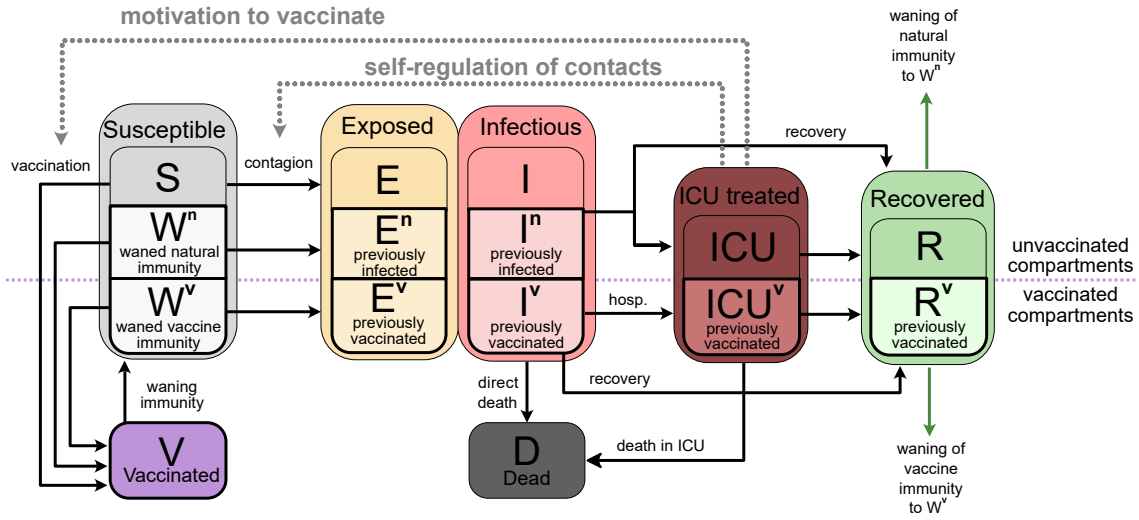

Supplementary Figure S1: **Age-stratified SEIRD-ICU compartmental model with vaccination and feedback loops for the interplay between information and disease spread.** Besides considering relevant compartments to capture COVID-19 dynamics, we explicitly incorporate mechanisms of voluntary preventive action through behavioural changes in response to information and individual perception of risks. We incorporate two mechanisms of voluntary action: (i) individuals can voluntarily adapt their immediate health-protective behaviour, adapting it according to their possibilities and the risk they perceive, and (ii) adapt their willingness regarding vaccination, being likelier to accept vaccine offers when feeling at risk for prolonged periods. Transition rates and other variables are listed in Tables S3 and S5, but omitted in the figure for clarity purposes.

We model the spreading dynamics of SARS-CoV-2 by a deterministic age-stratified compartmental model. Our model incorporates disease spreading dynamics (SEIRD), intensive care unit stays (ICU), the roll-out of a single-dose equivalent vaccine and boosters thereof (V), the protection from which wanes over time, and the interplay between risk perception and disease spread through the self-regulation of voluntary health-protective behaviour. We assume that health-protective behaviour is modulated by the perception of risk. When perceiving risks, humans tend to weigh more recent developments more heavily as well as put more weight on developments in the timescale relevant for the decision to be made (i.e., shorter timescales for immediate actions and longer ones for one-time decisions with sustained consequences) Zauberman et al. (2009). Explicitly, if perceiving increased risk, individuals can (i) adapt their level of potentially contagious contacts they have

and (ii) adapt their willingness towards seeking vaccination. For a graphical representation of the dynamics see Fig. S1.

In our model, susceptible (S) individuals can acquire the virus from infected individuals and subsequently progress to the exposed ($S \to E$) and, after the latent period, to the infectious ($E \to I$) compartment. Vaccinated and recovered individuals can be infected after their immunity has waned. Alternatively, our model can be interpreted such that waning immunity increases the probability of breakthrough infections. Individuals whose natural or vaccine-induced immunity has waned are modelled via two compartments (W^n and W^v, respectively), which feature no protection against infection but against a severe course of the disease, i.e., have reduced probabilities of requiring intensive care or dying. If infected, they transit to different exposed (E^n, E^v) and infectious (I^n, I^v) compartments so that vaccinated and unvaccinated individuals are separated.

The infectious compartments have three different possible transitions: i) direct recovery ($I, I^n \to R$ and $I^v \to R^v$) with rate γ, ii) admission to ICU ($I, I^n \to \mathrm{ICU}$ and $I^v \to \mathrm{ICU}^v$) with rate δ (reduced by a factor $(1-\kappa)$ for I^n, I^v) or iii) direct death ($I, I^n, I^v \to D$) with rate θ (reduced by a factor $(1-\kappa)$ for I^n, I^v). We assume the recovery and death rate in ICU to be independent of immunisation status. That way, individuals receiving ICU treatment either recover at a rate γ_{ICU} ($\mathrm{ICU} \to R$ and $\mathrm{ICU}^v \to R^v$) or die at a rate θ_{ICU} ($\mathrm{ICU}, \mathrm{ICU}^v \to D$). Note that the probability to get admitted to an ICU is reduced for infected individuals with waned immunity. However, their death rate in ICU is equal to that of those infected for the first time. We use two ICU compartments to separate the vaccinated from the unvaccinated compartments to keep track of individuals who can still receive a vaccine after recovering.

Each compartment is split into sub-compartments for the age groups that interact with each other following the contact matrix described in Sec. S1.2. Full age-structured model equations are presented in Sec. S3. Apart from the transmission-relevant interactions, the effect of having different age groups is incorporated into our vaccine feedback (described in Sec. S2.1) as well as in the transition rates between compartments (described in Sec. S2.2).

S1.1 Memory kernel

In this section we specify the memory kernel that measures how risk perception builds on past development of the ICU occupancy. These memory kernels (Fig. S2) relate to two processes occurring on different timescales. Voluntary adaption of health-protective behaviour depends on the perceived risk in the recent past, $H_R(t)$, defined as:

$$H_R(t) := \mathrm{ICU}^{\mathrm{tot}} * \mathcal{G}_{p_R,b_R} = \int_{-\infty}^{t} \mathrm{dt}' \, \mathrm{ICU}^{\mathrm{tot}}(t') \, \mathcal{G}_{p_R,b_R}(-t'+t) \, . \tag{1}$$

$\mathrm{ICU}^{\mathrm{tot}}(t)$ is the sum of all patients in ICU treatment at time t: $\mathrm{ICU}^{\mathrm{tot}}(t) = \sum_i \mathrm{ICU}_i(t) + \mathrm{ICU}_i^v(t)$. The arguments of the Gamma distribution $\mathcal{G}_{p_R,b_R}$ are set to $p_R = 0.7$ (shape) and $b_R = 4$ (rate), resulting in a curve that peaks at around four days in the past (Fig. S2a). Depending on $H_R(t)$, individuals reduce their potentially contagious contacts in different contexts by a weighting factor $k_{\mathrm{NPI,self}}$ (Fig. 2, main text) within thresholds determined by current mandatory NPIs (Fig. S3). See Sec. S4 for a sensitivity analysis on parameter choices.

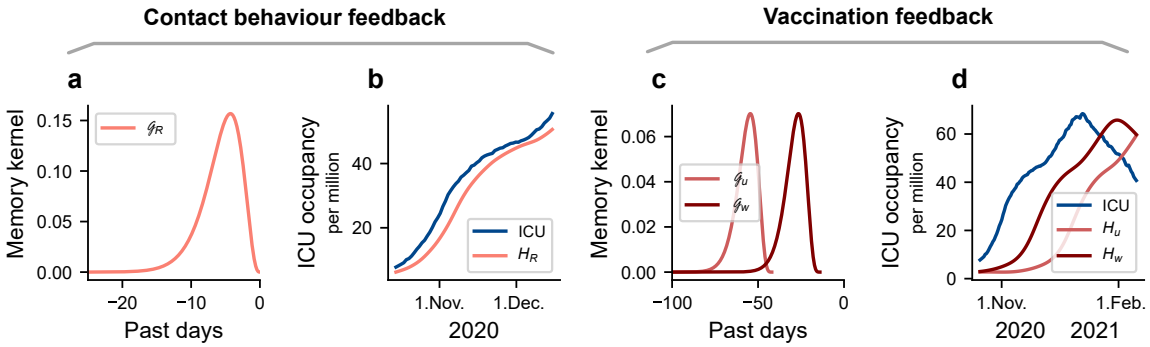

Supplementary Figure S2: **Modelling the relationship between perceived risk and pandemic developments.** Based on the information that individuals receive on the recent developments of the pandemic (e.g., ICU occupancy), they form their perception of risk. The way individuals perceive these temporal trends is biased towards recent developments, prioritising them over past developments for their decisions Zauberman et al. (2009). Furthermore, we assume a delay in individuals' reactions to ICU occupancy because of (i) delays inherent to the information spreading dynamics, and (ii) need for recurrent stimuli and various sources for accepting new information. Therefore, we convolve the ICU occupancy time series with a Gamma delay kernel (**a**), which captures both the delay related to information delivery and the subjective perception of time described above. Vaccine dynamics require a further delay related to the time required to build up immunity: Individuals whose immunity takes effect at a certain time made their decision and got vaccinated some time ago. The length of this delay depends on whether it is a first time or booster vaccination (**c**). **b,d:** Once convoluted with ICU occupancy (German example shown here), we obtain a measure for perceived risk H_R, H_u and H_w, respectively, for the voluntary adaption of immediate health-protective behaviour, first-time vaccination, and booster vaccination. In comparison with the actual ICU development, the variables H_* are smoother and delayed in time, representing non-instantaneous decisions based on individuals' perception of the recent ICU occupancy.

Time memory for vaccination willingness is assumed to work in the same way, but with different Gamma distributions, for two reasons. Firstly, there is a delay τ_u or τ_w between the decision to be vaccinated and the onset of immunity. Secondly, vaccination willingness is assumed to depend more strongly on past ICU occupancy compared to more immediate health-protective behaviour. Combined, it translates into a Gamma distribution $\mathcal{G}_{p_{\text{vac}},b_{\text{vac}}}$ that is shifted in time and is flatter (Fig. S2c), which is characterised by the parameters τ_u, τ_w, $p_{\text{vac}} = 0.4$ and $b_{\text{vac}} = 6$:

$$H_{u,w}(t) := \text{ICU}^{\text{tot}} * \mathcal{G}_{p_{\text{vac}},b_{\text{vac}}} = \int_{-\infty}^{t} \text{dt}' \, \text{ICU}^{\text{tot}}(t') \, \mathcal{G}_{p_{\text{vac}},b_{\text{vac}}}(-t' - \tau_{u,w} + t). \tag{2}$$

The subscripts u and w indicate first and booster doses, respectively. Booster doses are usually only a single dose so τ_w is just the delay between administration of the dose and onset of immunity, which we assume to be 2 weeks. The parameter τ_u is larger than τ_w because we include the delay of around 6 weeks for most vaccines that need two doses. For the initial conditions of H_R and $H_{u,w}$, ICU and ICU^v are set to a constant $\text{ICU}(t < 0) = \text{ICU}(t = 0)$ (same for ICU^v) in the past.

S1.2 Spreading dynamics

In our model, the spreading dynamics are governed by the sizes of the infectious compartments I, I^n, I^v and the compartments S, W^n, W^v, from which a transition to an infected state is possible. We include the effects of (i) mandatory non-pharmaceutical interventions (NPIs), (ii) individuals voluntarily adapting their health-protective behaviour based on perceived risk, and (iii) seasonality. Each is represented by a factor k that acts as a multiplicative reduction or increase on the spreading dynamics.

Seasonality is described by the factor $k_{\text{seasonality}}$ (see Equation 7 below). Mandatory NPIs and individuals' voluntary preventive actions are represented by $k_{\text{NPI,self}}(H_R)$. It does not factorise into single contributions of mandatory NPIs and voluntary preventive action because we assume the level of NPIs and voluntary behaviour to be coupled.

We introduce an infection term $\sum_j C_{ji}\mathcal{I}_j$ that governs the spreading between age groups i and j. The term is present in all differential equations that include transmissions, i.e., the transitions

$$\begin{array}{ll} S_i \to E_i & \text{non vaccinated, non infected} \\ W_i^n \to E_i^n & \text{waned infected (unvaccinated)} \\ W_i^v \to E_i^v & \text{waned vaccinated (potentially infected previously)} \end{array} \quad . \tag{3}$$

include a term proportional to $\sum_j C_{ji}\mathcal{I}_j$, which is subtracted from the susceptible and waned and added to the exposed states.

C_{ij} is the overall contact matrix, which we describe below, and $\mathcal{I}_i$ is a term describing the infectiousness of age group i. We define it as

$$\mathcal{I}_i := \beta \cdot k_{\text{seasonality}} \cdot \frac{I_i^{\text{eff}}}{M_i} \quad \text{with} \quad I_i^{\text{eff}} := (I_i + I_i^n + I_i^v + \Psi M_i) \; . \tag{4}$$

β is the spreading rate, I^{eff} is the effective size of the infectious compartments, M_i is the total population size of age group i, and Ψ is an external influx of infections, which we assume to be distributed equally over the population, e.g., being the largest for the largest age group.

The coupling between age groups is represented by a pre-COVID-19 contact matrix C_{ij}. This matrix represents the static, non-ICU-dependent contact behaviour of the different age groups (age group i potentially infecting age group j). It can be interpreted as the sum of various layers of contextual contacts (work-, school-, community-, and household-related contacts) Mistry et al. (2021). For a graphical representation of the contextual layers, see Fig. 1, main text, and Fig. S3. Depending on the context, some of these contacts can be voluntarily reduced according to individuals' perception of risk. Hence, we use each of the contextual layers of the matrix C_{ij}^{ν} separately and weigh each layer with reduction factors $k_{\text{NPI,self}}^{\nu}(H_R)$. We use H_R as an effective measure of the ICU occupancy that reflects the population's perceived risk (see subsection S1.1). Finally, we normalise the overall contact matrix C_{ij} by its spectral radius when its values are not reduced because of mandatory NPIs or voluntary protective behaviour, i.e., at $k_{\text{NPI,self}} = 1$ and $H_R = 0$. That way, the largest eigenvalue of the contact matrix $C_{ij} = \sum_\nu C_{ij}^{\nu}$ equals one in the absence of mandatory NPIs and voluntary measures.

The resulting infection term present in all transmission-related differential equations for age group i is thus

$$\sum_j C_{ji}\mathcal{I}_j = \beta \cdot k_{\text{seasonality}} \sum_j \left(\sum_\nu C_{ji}^{\nu} \cdot k_{\text{NPI,self}}^{\nu} \right) \frac{I_j^{\text{eff}}}{M_j} \, , \tag{5}$$

with j counting age groups and ν counting layers of the contact matrix. Having a normalised contact matrix C_{ij}, we can approximate the seasonal reproduction number $R_{0,\text{seasonal}}(t)$, which is defined as the largest eigenvalue of the next generation matrix Diekmann et al. (2010), at $H_R = 0$. By assuming that $\delta, \theta \ll \gamma$, we get

$$R_{0,\text{seasonal}}(t) \approx k_{\text{seasonality}}(t)\frac{\beta}{\gamma}\,, \tag{6}$$

with $\gamma = \sum_i \gamma_i M_i$. Postulating that $R_0 = 5$ at $k_{\text{seasonality}} = 1$, we can use this formula to calculate the spreading rate β. Note that this only holds true if seasons are long compared to the duration of an infection. With the latent period being $\frac{1}{\rho} = 4$ days and the duration in the infected compartment approximately $\frac{1}{\gamma} = 10$ days, the duration of an infection is roughly two weeks which is shorter than the time scale over which seasonality varies significantly.

We incorporate the effect of seasonality $k_{\text{seasonality}}$ as a time-dependent sinusoidal modulation factor, as proposed in Gavenčiak et al. (2021):

$$k_{\text{seasonality}} = 1 + \mu \cos\left(2\pi \frac{t + d_0 - d_\mu}{360}\right), \tag{7}$$

where μ is the sensitivity to seasonality, d_0 the starting day of the simulation, and d_μ the day with the highest effect on seasonality. We set $d_\mu = 0$, corresponding to January 1st. For simplicity, we assume that one month has 30 days and a full year, thus, 360 days. This approximation does not affect the results in the observed time horizon.

S1.3 Contact matrices

In our model, individuals can adapt the level of contagious contacts based on their perception of risk. Explicitly, we consider the contact matrices for the German population reported in Mistry et al. (2021), which differentiate between four different contexts (Households, Schools, Workplaces, and Communities). These matrices are represented in Fig. S3a, c, e, g. Then, depending on the perception of risk, the scenario of mandatory NPIs, and how much freedom these allow for in different contexts, we calculate a weighting factor $k_{\min} \leq k^{\nu}_{\text{NPI,self}}(H) \leq k_{\max}$ that multiplies each matrix (Fig. S3b, d, f, h). Scenario-dependent threshold values for the weighting factors are reported in Table 1 and explained in the Methods Section, main text.

The contact matrix for the Community context is equally distributed, meaning that each individual ("x-axis") has the same probability of being infected by any contact ("y-axis"), independent of age. Because the age groups are different in size, a horizontal pattern emerges; it is likelier to be infected by an individual part of a larger age group.

Although straightforward to understand, the household layer of contacts applied to our mean-field model may lead to unrealistic results in some situations. For example, consider an ideal full lockdown policy where any transmissions between households were perfectly eliminated. Obviously, in such a theoretical scenario, the pandemic would quickly end as infected individuals would not transmit the virus any further than to contacts within their household. However, under a mean-field

compartmental model, the distinction between people in one's household and another household cannot be made, which would lead to a viral spread even under such a scenario. To solve this issue, the factor $k^{\text{Households}}_{\text{NPI,self}}(H)$ is scaled by a factor which is the average of the other reductions: $\frac{1}{3}\sum_{\nu} k^{\nu}_{\text{NPI,self}}(H)\,, \nu \in \{\text{Schools, Workplaces, Communities}\}$. In that way, eliminating all contacts in contexts aside from households should end the pandemic.

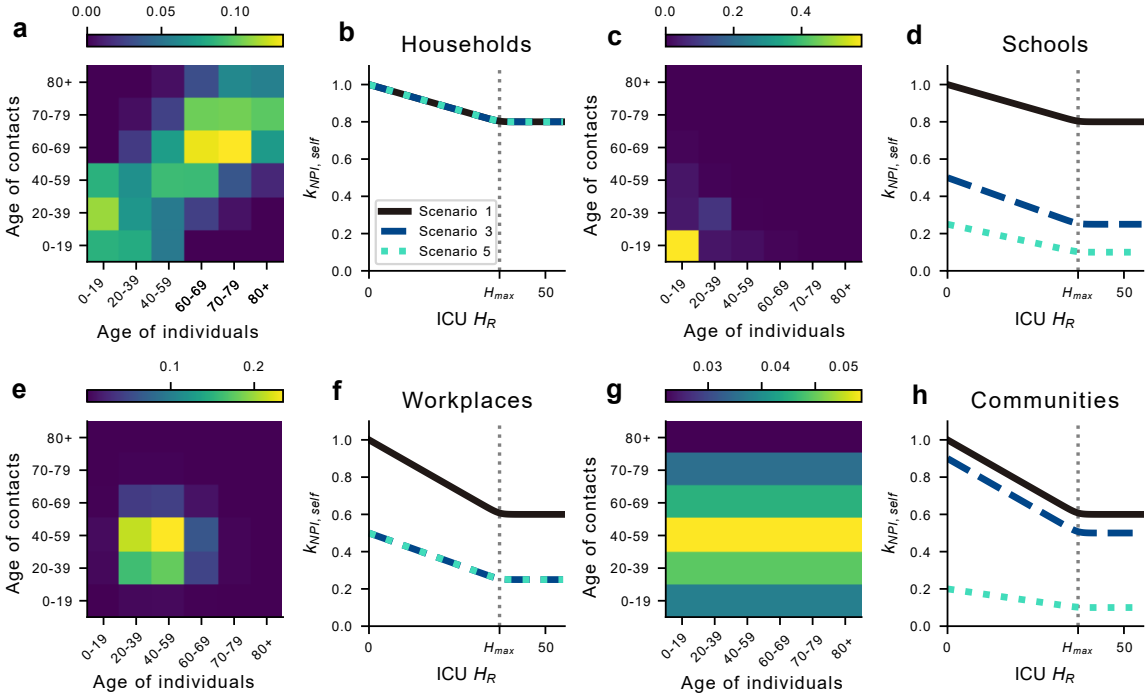

Supplementary Figure S3: **The mechanism of the reduction of potentially contagious contacts.** The contact matrix for interactions within households, schools, workplaces and communal activities (**a,c,e,g**) and the ICU-occupancy-dependent reduction $k^{\nu}_{\text{NPI,self}}(H_R)$ (**b,d,f,h**) for scenarios 1,3, and 5. Each matrix entry is multiplied by the value of $k^{\nu}_{\text{NPI,self}}(H_R)$ (**b,d,f,h**), which decreases linearly with perceived ICU occupancy H_R up to the point $H_{max} = 37$ where no further reduction is taken as motivated by Fig. 2, main text.

S1.4 Vaccination effects and waning immunity

Our model includes the effect of vaccination, where vaccines are for simplicity administered with a single-dosage delivery scheme. Vaccinated individuals cannot be infected while being in the vaccinated compartment, but will proceed to the waned immunity compartment W^v at a rate Ω Thomas et al. (2021); Puranik et al. (2021). The same applies to recovered individuals, who also lose their post-infection immunity at rate Ω Turner et al. (2021). Hence, people transition from compartment R_i to compartment W^n_i and from R^v_i and V_i to W^v_i at rate Ω.

We assume the emptying of the immune compartments to be exponential with rate Ω or, equivalently, with half-life period $T_{1/2} = \ln(2)/\Omega$. In other words, we assume that after $T_{1/2}$, half of the immune individuals have completely waned immunity and the other half is still fully immune. Within the mean-field approximation, this corresponds to all individuals in the immune compartments having halfway waned immunity after $T_{1/2}$. This time, when the effectiveness against infection η reduces to 50%, equals to about 5 months according to empirical data (for vaccination)

Tartof et al. (2021). Hence, the waning immunity rate is given by

$$\Omega = \frac{\ln(2)}{T_{1/2}} \approx \frac{\ln(2)}{5 \cdot 30\,\text{days}} \approx \frac{1}{225}\frac{1}{\text{days}}. \tag{8}$$

As soon as individuals enter one of the waned compartments they can be infected with the same probability as individuals never infected or vaccinated before. However, we assume that robustness against a severe course of the disease remains high Tartof et al. (2021); Chemaitelly et al. (2021); Pegu et al. (2021); Naaber et al. (2021) which leads to a reduction of $(1-\kappa)$ to the probability of requiring treatment in ICUs or dying directly. The parameter κ is estimated using κ_{obs}, which denotes the full protection against hospitalisation as in observed studies. The parameter κ used in our model is lower than κ_{obs} because it is the effectiveness against hospitalisation once an individual is already infected. We estimate it via

$$(1-\eta)(1-\kappa) = (1-\kappa_{\text{obs}}) \tag{9}$$

with η being the vaccine effectiveness against an infection. According to Tartof et al. (2021) it holds that $\eta = 0.5$ and $\kappa_{\text{obs}} = 0.9$ (both after five months). Thus, we estimate $\kappa \approx 0.8$ and approximate it to be independent of the time after vaccination.

S1.5 Vaccine uptake

The age group dependent vaccine uptake is described by two different functions: one for susceptible individuals (ϕ_i) and one for individuals whose immunity has waned (φ_i). The core idea is to vaccinate only if willingness for vaccine uptake is larger than the fraction of already vaccinated; if the fraction of individuals who are willing to be vaccinated with a first dose (u^{willing}) is larger than the fraction of already vaccinated (u^{current}), vaccinations are carried out at a rate proportional to the difference of the two.

Willingness to be vaccinated depends on the past development of the ICU occupancy numbers. u^{willing} can shift between a minimum and a maximum value (u^{base} and $u^{\text{max}} = 1 - \chi_u$), representing the general observed acceptance for the first dose and people who are strictly opposed to vaccines or cannot be immunised because of age or other preconditions (making up χ_u), respectively. The sensitivity constant α_u determines how sensitive to ICU occupancy the vaccine hesitancy is (see Sec. S1.5.1). The willingness to receive the first dose of the vaccine is then described by

$$u_i^{\text{willing}} = u_i^{\text{base}} + \left(u_i^{\text{max}} - u_i^{\text{base}}\right)\left(1 - \exp\left(-\alpha_u H_u\right)\right). \tag{10}$$

Hence, u_i^{willing} is a fraction for each age group i between zero and one and the total number of people willing to be vaccinated in each age group i is thus $u_i^{\text{willing}} M_i$. For the differences in the parameters u_i^{base} and $u_{i,\text{max}}$ between age groups, see Sec. S2.1 and for a graphical example representation of u^{willing} see Fig.2e, main text.

The function that determines the rate at which first time vaccines are administered is denoted by ϕ. It determines the transition away from S_i and W_i^n, is age group dependent, and is described via a softplus function:

$$\phi_i(H_u) = \frac{1}{t_u} \cdot \frac{S_i + W_i^n}{M_i(1 - u_i^{\text{current}})} \cdot \epsilon \ln\left(\exp\left(1 + \frac{1}{\epsilon}\left(u_i^{\text{willing}}(H_u) - u_i^{\text{current}}\right)\right)\right), \tag{11}$$

where ϵ is a curvature parameter. Multiplying by $\frac{S_i+W_i^n}{M_i(1-u_i^{\text{current}})}$ ensures that we only vaccinate if people are actually present in S or W^n. Dividing by t_u smoothens the transition between the state of vaccinating and not vaccinating, the physical explanation being that people require time (of the order of t_u days) to organise a vaccine, which reduces the vaccination rate after crossing the threshold. t_u is assumed to be constant here. However, when there is a lot of demand for vaccine uptake, t_u is likely larger in reality due to administrative and logistical problems. For the implementation of ϕ_i into the model equations, see Sec. S3. In the term $\frac{dS_i}{dt}$ we multiply ϕ by $\frac{S_i}{S_i+W_i^n}$ and in the term $\frac{dW_i^n}{dt}$ we multiply by $\frac{W_i^n}{S_i+W_i^n}$, effectively splitting up the vaccinations among the two groups.

The administration of booster doses works in a similar way. First, we define a function for the age group dependent willingness to accept a booster dose:

$$w_i^{\text{willing}} = w_i^{\text{base}} + \left(w_i^{\text{max}} - w_i^{\text{base}}\right)\left(1 - \exp\left(-\alpha_w H_w\right)\right). \tag{12}$$

The function for booster doses φ can then be written as

$$\varphi_i(H_w) = \frac{1}{t_w} \cdot \frac{W_i^v}{M_i(u_i^{\text{current}} - w_i^{\text{current}})} \cdot \epsilon \ln\left(\exp\left(1 + \frac{1}{\epsilon}\left(w_i^{\text{willing}}(H_w)u_i^{\text{current}} - w_i^{\text{current}}\right)\right)\right), \tag{13}$$

We only vaccinate if willingness among those who received a first dose is larger than the fraction of already boostered people, i.e. u_i^{current} is the upper limit for w_i^{current}.

S1.5.1 Assessment of sensitivity to ICU occupancy for vaccination dynamics

In our model, we assume the willingness in the total population to be vaccinated for the first time to range between threshold values u^{base} and u^{max}. The difference $u^{\text{max}} - u^{\text{base}}$ is the fraction of people that, initially hesitant, decide to accept the vaccine offer based on their perception of risk. In order to estimate how sensitive this group is to risk perception in the form of awareness about the ICU occupancy, we proceed as follows. If we estimate the ICU occupancy at which half of the people belonging to this initially hesitant group accepts a vaccination, we can calculate the sensitivity parameter α_u: Let $H_{1/2}$ be this ICU occupancy. We then have to solve

$$u^{\text{base}} + \frac{1}{2}\left(u^{\text{max}} - u^{\text{base}}\right) \stackrel{!}{=} u^{\text{base}} + \left(u^{\text{max}} - u^{\text{base}}\right)\left(1 - \exp\left(-\alpha_u H_{1/2}\right)\right), \tag{14}$$

which reduces to

$$\alpha_u = \frac{\log 2}{H_{1/2}}. \tag{15}$$

We assume $H_{\max}$, i.e., the threshold at which no further adaption of health-protective behaviour occurs, as a first estimate for $H_{1/2}$ to obtain an approximate value for the sensitivity as $\alpha_u = \frac{\log 2}{H_{\max}} = \frac{\log 2}{37} \approx 0.02$. The quantified effect that this parameter has on the results is explored in Sec. S4.

S1.5.2 Tracking vaccinated individuals

Transition rates between the susceptible (S_i) and waned (W_i^n, W_i^v) compartments due to vaccination depend on the difference between willingness to be vaccinated and the fraction of currently vaccinated. Thus, it is necessary to keep track of how many people have received a first and booster dose, respectively. This is modelled by integrating over the vaccination rates. It translates into two additional differential equations:

$$\frac{d}{dt} u_i^{\text{current}} = \phi_i(H_u) \quad \text{and} \quad \frac{d}{dt} w_i^{\text{current}} = \varphi_i(H_w)\,, \tag{16}$$

where u^{current} and w^{current} are the fraction of people who received a first and booster dose, respectively. The initial conditions for u_i^{current} and w_i^{current} are the total reported numbers of administered vaccine doses Ritchie et al. (2021).

S1.6 Exploring vaccination rate and ICU occupancy trends in different European countries

The main assumption underlying the vaccination feedback is that vaccination willingness follows ICU occupancy. In the case of Romania this relation is evident (Figure S4): Approaching winter 2021, case numbers and ICU occupancy had a steep rise, arguably due to insufficient immunity among the population, as vaccine coverage was under 30% Ritchie et al. (2021). Under such circumstances, there was a lot of "room for improvement" within the unvaccinated population not strictly opposed to vaccines, which led to a steep surge in administered doses (Fig. S4). Note that there might also be other underlying causes for increased vaccine uptake: For example, imposing restrictions only onto unvaccinated might motivate vaccine uptake. While this is a governmental choice not considered in our model, such enforcements usually follow high levels of ICU occupancy and are thus indirectly accounted for.

In countries other than Romania, the trend is less visible (Fig. S4). Several countries show an increase in vaccine uptake in October 2021; however, it is unclear whether this is mainly motivated by voluntary behaviour following an increase in ICU occupancy. Concurrently, requests for launching country-wide booster campaigns were on the rise, which might have been the leading cause of increased vaccine uptake. However, whether the causes are voluntary behaviour or institutional recommendations regarding vaccinations, both follow perceived risk (on individual level vs governmental level) and lead to the same effect: increased ICU occupancy leads to increased vaccine uptake. Apart from Estonia and Belgium, we do not observe countries in which a rise in ICU occupancy is not followed by a rise in vaccinations. If the contrary is the case, i.e., vaccines

rising despite ICU occupancy staying low, this could be attributed to external motivations and would require further country-specific investigation.

In countries where we observe increasing vaccines following ICU occupancy, we should note that the delay between the two varies a lot. While in Romania and Bulgaria, the delay seems to be of the order of one month, we observe that in Germany, Austria and the Czech Republic, there does not seem to be any relevant delay. Note that the vaccination curve measures daily administered vaccines and not the onset of immunity (which the kernel in our model represents). The effect of the delay incorporated in our model is quantified in the sensitivity analysis S4.

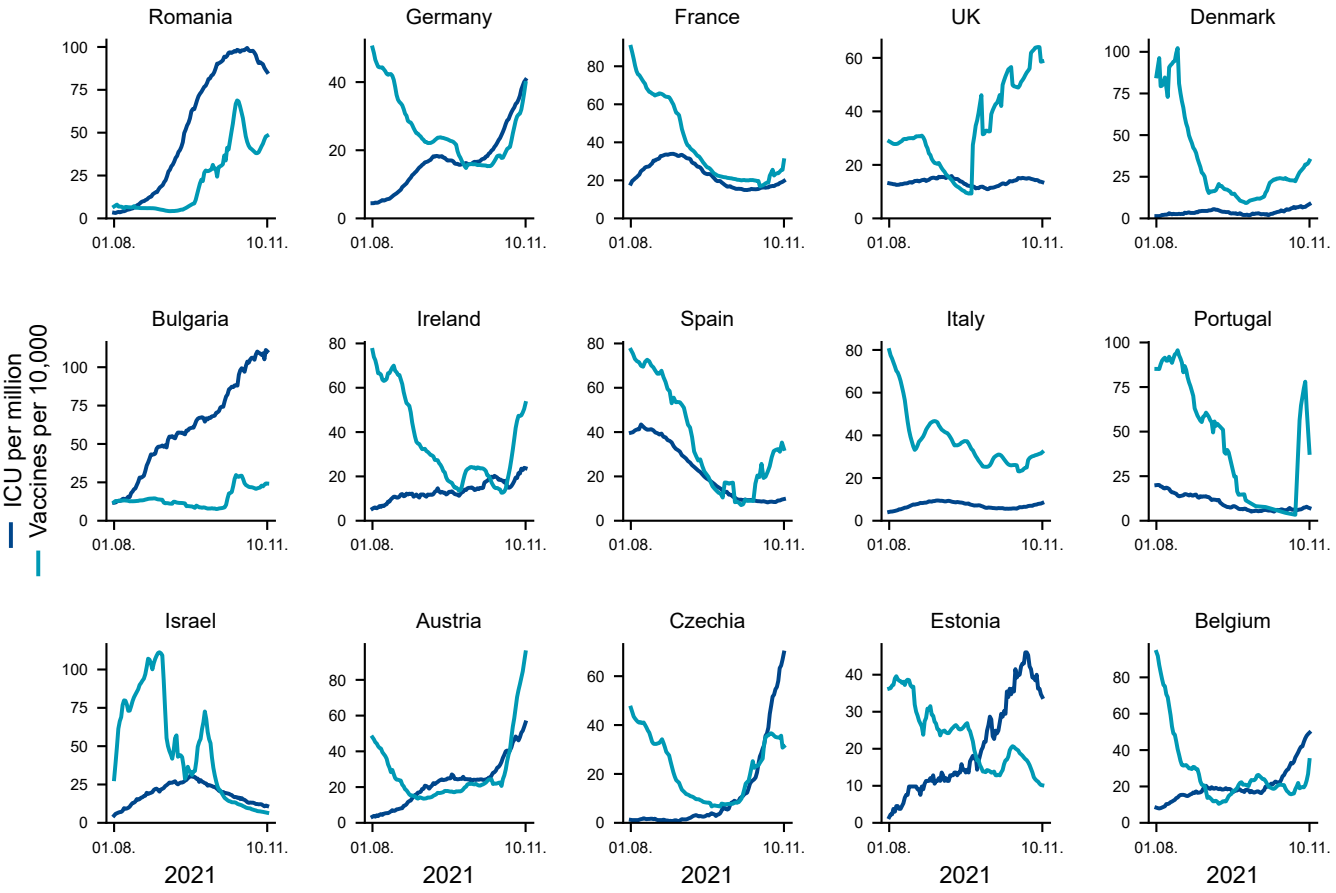

Supplementary Figure S4: **Vaccination rate and ICU occupancy trends across selected countries.** ICU occupancy per million inhabitants and daily vaccinations per 10,000 inhabitants for several European countries and Israel. Booster doses and first time doses are added together.

S2 AGE STRATIFICATION

S2.1 Age-dependent vaccine uptake

Although there are vaccines accredited for children below 12 years in the European Union, we assume that these age groups will have much lower uptakes, affecting our parameters $u_i^{\max}$ (maximum vaccine uptake) and $w_i^{\max}$ (maximum booster uptake). Furthermore, due to likelier side effects of vaccines for the young, but lesser consequences of an infection, we assume that these parameters as well as the baseline acceptances for vaccines increase with age. Thus, u_i^{base}, w_i^{base}, $u_i^{\max}$ and $w_i^{\max}$

become age-dependent. All vaccine-related parameters are listed in Table S1. Note that $w_i^{\max}$ is a fraction of u_i^{current} and not of M_i, thus it is no contradiction if $w_i^{\text{base}} > u_i^{\text{base}}$.

Table S1. Different age groups and age-dependent parameters related to vaccine uptake.

Group ID	age group	fraction of population M_i/M	$u_i^{\max}$	$w_i^{\max}$	u_i^{base}	w_i^{base}
1	0-19	0.18	0.35	0.76	0.2	0.1
2	20-39	0.25	0.9	0.8	0.5	0.25
3	40-59	0.28	0.92	0.84	0.55	0.275
4	60-69	0.13	0.94	0.88	0.6	0.3
5	70-79	0.09	0.96	0.92	0.65	0.325
6	80+	0.07	0.98	0.96	0.7	0.35

S2.2 Age-dependent transition rates

Differing disease severity after a SARS-CoV-2 infection for different age groups translates into age-dependent transition rates between our model compartments. More specifically, we include age-dependent parameters for the natural recovery rate γ, the ICU admission rate δ, the death rate θ and the recovery as well as death rates from ICU, γ_{ICU} and θ_{ICU}, respectively. Table S2 lists the different parameters as reported in Bauer et al. (2021).

Table S2. Age-dependent transition parameters related to the ICU-, death- and recovery rates. All parameters are given in units of days^{-1}.

ID	Age group	Recovery rate γ_i $\left[\text{day}^{-1}\right]$	ICU adm. rate δ_i $\left[\text{day}^{-1}\right]$	Death rate θ_i $\left[\text{day}^{-1}\right]$	ICU rec. rate $\gamma_{\text{ICU},i}$ $\left[\text{day}^{-1}\right]$	ICU death rate $\delta_{\text{ICU},i}$ $\left[\text{day}^{-1}\right]$
1	0-19	0.09998	0.000014	0.000002	0.19444	0.00556
2	20-39	0.09978	0.000204	0.000014	0.19222	0.00778
3	40-59	0.09867	0.001217	0.000111	0.084745	0.006164
4	60-69	0.09565	0.004031	0.000317	0.081401	0.009508
5	70-79	0.09314	0.005435	0.001422	0.091355	0.019756
6	80+	0.08809	0.007163	0.004749	0.084233	0.082433

S3 MODEL EQUATIONS

The combined contributions of the infection-spreading and vaccination dynamics are represented by the set of equations below. The time evolution of our model is then completely determined by the initial conditions of the system. The first-order transition rates between compartments are given by the probability for an individual to undergo this transition divided by the average transition time, e.g., the recovery rate γ is the probability that an individual recovers from the disease divided by the time span of the recovery process. Note that in principle γ should be different for the I and I^B compartment, as the probability to recover is larger for individuals previously immunised. We neglect this difference as it is negligible within the margin of error since the probability to recover is close to 1 in both cases. The subscripts i denote the sub-compartments for each age group and C_{ij} the contact matrix that describes the interactions within the age groups.

$$I_i^{\text{eff}} = \underbrace{(I_i + I_i^n + I_i^v + \Psi M_i)}_{\text{effective incidence}} \tag{17}$$

$$\mathcal{I}_i = \underbrace{\beta\, k_{\text{seasonality}}\, \frac{I_i^{\text{eff}}}{M_i}}_{\text{effective infection rate}} \tag{18}$$

$$C_{ij} = \underbrace{\sum_{\nu} C_{ij}^{\nu}\, k_{\text{NPI,self}}^{\nu}}_{\text{sub-matrices times reductions}} \tag{19}$$

$$\frac{dS_i}{dt} = -\underbrace{S_i \sum_j C_{ji}\mathcal{I}_j}_{\text{unvaccinated infections}} - \underbrace{M_i \phi_i(H_u) \frac{S_i}{S_i + W_i^n}}_{\text{first vaccinations}} \tag{20}$$

$$\frac{dW_i^n}{dt} = -\underbrace{W_i^n \sum_j C_{ji}\mathcal{I}_j}_{\text{waned infections}} - \underbrace{M_i \phi_i(H_u) \frac{W_i^n}{S_i + W_i^n}}_{\text{first vaccinations}} + \underbrace{\Omega R_i}_{\text{waning natural immunity}} \tag{21}$$

$$\frac{dW_i^v}{dt} = -\underbrace{W_i^v \sum_j C_{ji}\mathcal{I}_j}_{\text{waned infections}} - \underbrace{M_i u_i^{\text{current}} \varphi_i(H_w)}_{\text{booster vaccinations}} + \underbrace{\Omega V_i + \Omega R_i^v}_{\text{waning immunity}} \tag{22}$$

$$\frac{dV_i}{dt} = \underbrace{M_i \left(\phi_i(H_u) + u_i^{\text{current}} \varphi_i(H_w)\right)}_{\text{vaccinations}} - \underbrace{\Omega V_i}_{\text{waning vaccine immunity}} \tag{23}$$

$$\frac{dE_i}{dt} = \underbrace{S_i \sum_j C_{ji}\mathcal{I}_j}_{\text{unvaccinated exposed}} - \underbrace{\rho E_i}_{\text{end of latency}} \tag{24}$$

$$\frac{dE_i^n}{dt} = \underbrace{W_i^n \sum_j C_{ji}\mathcal{I}_j}_{\text{unvaccinated waned exposed}} - \underbrace{\rho E_i^n}_{\text{end of latency}} \tag{25}$$

$$\frac{dE_i^v}{dt} = \underbrace{W_i^v \sum_j C_{ji}\mathcal{I}_j}_{\text{vaccinated waned exposed}} - \underbrace{\rho E_i^v}_{\text{end of latency}} \tag{26}$$

$$\frac{dI_i}{dt} = \underbrace{\rho E_i}_{\text{start of infectiousness}} - \underbrace{(\gamma_i + \delta_i + \theta_i)\, I_i}_{\rightarrow\text{recovery, ICU, and death}} \tag{27}$$

$$\frac{dI^n}{dt} = \underbrace{\rho E_i^n}_{\text{start of infectiousness}} - \underbrace{(\gamma_i + (\delta_i + \theta_i)(1-\kappa))\, I_i^n}_{\substack{\rightarrow\text{recovery, ICU (reduced),} \\ \text{and death (reduced)}}} \tag{28}$$

$$\frac{dI_i^v}{dt} = \underbrace{\rho E_i^v}_{\text{start of infectiousness}} - \underbrace{(\gamma_i + (\delta_i + \theta_i)(1-\kappa))\, I_i^v}_{\substack{\rightarrow\text{recovery, ICU (reduced),} \\ \text{and death (reduced)}}} \tag{29}$$

$$\frac{d\mathrm{ICU}_i}{dt} = \underbrace{\delta_i \left(I_i + (1-\kappa) I_i^n\right)}_{\text{nonvaccinated ICU}} - \underbrace{(\gamma_{\mathrm{ICU},i} + \theta_{\mathrm{ICU},i})\mathrm{ICU}_i}_{\text{recovery or death in ICU}} \tag{30}$$

$$\frac{d\mathrm{ICU}_i^v}{dt} = \underbrace{\delta_i(1-\kappa) I_i^v}_{\text{vaccinated ICU}} - \underbrace{(\gamma_{\mathrm{ICU},i} + \theta_{\mathrm{ICU},i})\mathrm{ICU}_i^v}_{\text{recovery or death in ICU}} \tag{31}$$

$$\frac{dD_i}{dt} = \underbrace{\theta_i \left(I_i + (1-\kappa)\left(I_i^n + I_i^v\right)\right)}_{\text{death without ICU}} + \underbrace{\theta_{\mathrm{ICU},i} \left(\mathrm{ICU}_i + \mathrm{ICU}_i^v\right)}_{\text{death in ICU}} \tag{32}$$

$$\frac{dR_i}{dt} = \underbrace{\gamma_i (I_i + I_i^n)}_{\text{direct recovery}} + \underbrace{\gamma_{\mathrm{ICU},i}\, \mathrm{ICU}_i}_{\text{recovery}} - \underbrace{\Omega R_i}_{\substack{\text{waning} \\ \text{post-infection immunity}}} \tag{33}$$

$$\frac{dR_i^v}{dt} = \underbrace{\gamma_i I_i^v}_{\text{direct recovery}} + \underbrace{\gamma_{\mathrm{ICU},i}\, \mathrm{ICU}_i^v}_{\text{recovery from ICU}} - \underbrace{\Omega R_i^v}_{\substack{\text{waning} \\ \text{post-infection immunity}}} \tag{34}$$

$$\frac{du_i^{\text{current}}}{dt} = \underbrace{\phi_i(H_u)}_{\text{current first vaccinations}} \tag{35}$$

$$\frac{dw_i^{\text{current}}}{dt} = \underbrace{\varphi_i(H_w)}_{\text{current booster vaccinations}} \tag{36}$$

(37)

Table S3. Model parameters (in order of first appearance) related to infection dynamics. * :**Levin et al. (2020)Salje et al. (2020)Bauer et al. (2021)Linden et al. (2020)** The parameters referring to Table S2 are age-dependent.

Pa	Meaning	Value (default)	Unit	Source
γ	Recovery rate	Tab. S2	day^{-1}	He et al. (2020); Pan et al. (2020)
δ	Avg. hospitalisation rate ($I \to$ ICU)	Tab. S2	day^{-1}	*
κ	Reduction of hospitalisation rate (given infection) for individuals with waned immunity	0.8	–	Eq. 9
θ	Avg. death rate	Tab. S2	day^{-1}	*
γ_{ICU}	Recovery rate from ICU	Tab. S2	day^{-1}	*
θ_{ICU}	Avg. ICU death rate	Tab. S2	day^{-1}	*
C_{ij}	Contact matrix	–	–	Mistry et al. (2021)
β	Spreading rate	0.5	day^{-1}	Eq. 6
Ψ	Influx of infections	1	people/day	Assumed
R_0	Basic reproduction number (Delta variant)	5.0	–	Liu and Rocklöv (2021)
ρ	Rate of leaving exposed state	0.25	day^{-1}	Bar-On et al. (2020); Li et al. (2020)
μ	Sensitivity to seasonality	0.267	–	Gavenčiak et al. (2021)
d_0	Day when the time series starts	240	day	Chosen
d_μ	Day with the strongest effect on seasonality	0	day	Gavenčiak et al. (2021)
Ω	Waning immunity rate (base)	$\frac{1}{225}$	day^{-1}	Tartof et al. (2021), Eq. 8
η	Vaccine eff. against transmission 5 months after vaccination	0.5	–	Tartof et al. (2021)
κ_{obs}	Observed vaccine eff. against severe disease 5 months after vaccination	0.9	–	Tartof et al. (2021)

S3.1 Initial conditions

A primary task for defining the initial conditions is distributing the population size of $M = 10^6$ individuals onto our model compartments (Fig. S1). In reality, however, there are no well-defined compartments. For example, a person vaccinated a few months ago cannot be classified into either a V or W^n compartment, but is instead in a vaccinated state with reduced vaccine effectiveness. Furthermore, available data on vaccinated or infected individuals is often age-stratified by different age groups or not age-stratified at all. To approach these data challenges, we obtain the initial conditions through the following procedure (Fig. S5):

We postulate that we want to look at a population that is 60% vaccinated and 20% recovered (including the non reported cases). Let the resulting numbers of people be called $V^{\text{tot}} = 0.6M$ and $R^{\text{tot}} = 0.2M$, respectively. These values are inspired by the situation in Germany as of September 1st 2021. Next, we take German data on daily new infections N and ICU occupancy ICU^{tot} at this point in time Ritchie et al. (2021); am RKI (2020). These four values will be used to build all the

Table S4. Model parameters (in order of first appearance) related to the behavioural feedback loops. The range column describes the range of values used in the various scenarios.

Parameter	Meaning	Value (default)	Unit	Source
p_R, b_R	Shape and rate parameters of the memory kernel for the risk perception relevant to immediate health-protective behaviour, respectively	0.7, 4.0	–	Assumed
τ_u, τ_w	Memory time of the ICU capacity and delay to immunisation	2, 6	weeks	Assumed
p_{vac}, b_{vac}	Shape and rate parameters of the memory kernel for the risk perception relevant to vaccination, respectively	0.4. 6.0	–	Assumed
k^ν	Weighting factors for the contextual contact matrices	Tab. 1, main text	–	Assumed
$u^{\text{base}}, w^{\text{base}}$	Base fractions of vaccine acceptance (first and booster, respectively)	Tab. S1	–	Wouters et al. (2021)
χ_u, χ_w	Fraction of the population refusing vaccine (first and booster, respectively)	Tab. S1	–	Betsch et al. (2020)
α_u, α_w	Sensitivity of the population to ICU occupancy	0.02	people^{-1}	Eq. 15
ϵ	Curvature parameter for the softplus function describing the vaccination rate	1	–	Chosen
t_u, t_w	Organization time for vaccine (first and booster resp.)	7	days	Assumed
$H_{\max}$	Risk perception above which no further adoption of voluntary health-protective behaviour occurs	37	–	Fitted to Betsch et a

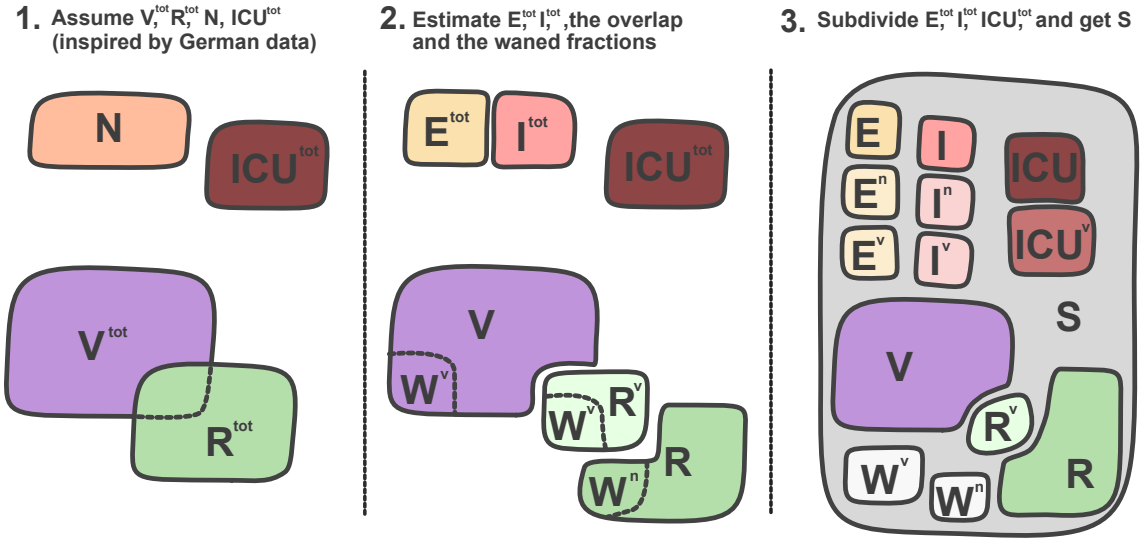

Supplementary Figure S5: **The procedure of obtaining initial conditions for the model compartments.** Starting with parts of the population attributed to different states N, ICU, V^{tot}, and R^{tot}, we calculate reasonable values for the initial conditions of all compartments step by step. Compartment sizes in the figure are chosen arbitrarily and do not represent actual size in terms of people.

other compartments. First, however, we have to uniformly age-stratify these values. ICU occupancy and the number of new COVID-19 cases can be obtained in an age-stratified way for the case of Germany. For the number of vaccinated and recovered, we assess countries that report age-stratified data, such as Denmark, and distribute the total numbers V^{tot} and R^{tot} onto the various age groups as can be seen in Tab. S6. Given the initial values for V_i^{tot}, R_i^{tot}, N_i and $\text{ICU}_i^{\text{tot}}$ for every age group i, we calculate the values for all other compartments:

Immune compartments separated by vaccination status and previous infection

First, we consider the possibility that individuals were both previously vaccinated and infected. Thus, to avoid overestimating the number of immunised individuals, we estimate the overlap between V_i^{tot} and R_i^{tot}: As a first order estimate, we assume that the probability of being vaccinated and having recovered are independent of each other. That way, the probability of being both vaccinated and recovered is given as the product of the two probabilities:

$$\text{Prob}(x \in V_i^{\text{tot}} \wedge x \in R_i^{\text{tot}}) = \text{Prob}(x \in V_i^{\text{tot}}) \cdot \text{Prob}(x \in R_i^{\text{tot}}) \tag{38}$$

Accordingly, the fraction of vaccinated in the total population for age group i, $\frac{V_i^{\text{tot}}}{M_i}$, is the same as the fraction of vaccinated in the recovered part of the population, $\frac{R_i^v}{R_i^{\text{tot}}}$. Hence, the initial numbers of recovered vaccinated, R_i^v, and unvaccinated individuals, R_i, are estimated via

$$R_i^v = \frac{V_i^{\text{tot}}}{M_i} R_i^{\text{tot}} \text{ and } R_i = R_i^{\text{tot}} - R_i^v. \tag{39}$$

Consequently, we receive the number of vaccinated individuals without previous infection by subtracting the overlap:

$$V_i = V_i^{\text{tot}} - R_i^v. \tag{40}$$

This process is illustrated in Fig. S5.

Waned compartments separated by immunity status

Next, we consider the fraction of vaccinated and recovered individuals whose immunity has waned (see Tab. S6): For the recovered, we assume that the time point at which infections took place in the past was age-independent and thus attribute the same fraction of waned natural immunity to all age groups. However, this assumption does not hold for vaccine-induced immunity because older age groups were typically vaccinated at an earlier point in time. We subtract the waned fractions from the compartments V_i, R_i and R_i^v, obtaining W_i^n and W_i^v.

Susceptible compartment

The susceptible compartment S_i comprises of all individuals not belonging to any of the other compartments. It can be calculated via

$$S_i = M_i - V_i - R_i - R_i^v - W_i^n - W_i^v - N_i - \text{ICU}_i^{\text{tot}}. \tag{41}$$

Exposed and infectious compartments separated by immunity status
We estimate the initial conditions for the exposed and infected compartments by first estimating $E_i^{\text{tot}} = E_i + E_i^n + E_i^v$ and $I_i^{\text{tot}} = I_i + I_i^n + I_i^v$ by

$$E_i^{\text{tot}} = \frac{1}{\rho} N_i \quad \text{and} \quad I_i^{\text{tot}} = \frac{1}{\gamma_i + \delta_i + \theta_i} N_i \,. \tag{42}$$

The fractions $\frac{1}{\rho}$ and $\frac{1}{\gamma+\delta+\theta}$ are the average times spent in the exposed and infected compartments, respectively (approximately).

To find out how E_i^{tot} and I_i^{tot} distribute onto their sub-compartments, i.e., for the different immune status and age groups, we look at their origin: Because all the infections in E_i originate from S_i, the ones in E_i^n from W_i^n and the ones in E_i^v from W_i^v, we can distribute E_i^{tot} onto the sub-compartments via

$$E_i = \frac{S_i}{S_i + W_i^n + W_i^v} E_i^{\text{tot}}, \quad E_i^n = \frac{W_i^n}{S_i + W_i^n + W_i^v} E_i^{\text{tot}}, \quad E_i^v = \frac{W_i^v}{S_i + W_i^n + W_i^v} E_i^{\text{tot}} \tag{43}$$

and analogously for I_i^{tot}.

ICU compartments separated by vaccination status
To determine the distribution of $\text{ICU}_i^{\text{tot}}$ onto the compartments ICU_i and ICU_i^v, we consider that the probability to require ICU care for individuals in the compartments I_i^n and I_i^v is reduced by a factor of $(1-\kappa)$. Hence,

$$\text{ICU}_i^v = \frac{I_i^v(1-\kappa)}{I_i + (I_i^n + I_i^v)(1-\kappa)} \text{ICU}_i^{\text{tot}} \quad \text{and} \quad \text{ICU}_i = \text{ICU}_i^{\text{tot}} - \text{ICU}_i^v. \tag{44}$$

The initial condition for the dead is set to $D_i = 0$, for the currently vaccinated to $u_i^{\text{current}} = V_i^{\text{tot}}$ and for the currently boostered to $w_i^{\text{current}} = 0$. For the initial condition of H_*, values of past ICU occupancy development are needed. Here, we assume a constant past value of the ICU occupancy at $t \leq d_0$ for both ICU compartments.

S4 SENSITIVITY ANALYSIS

The results of this model depend on the choices of all parameters involved. While some epidemiological parameters are well understood and quantified at this point in the pandemic, some other parameters of our model remain uncertain, but might have a large impact on the results. In this section we analyse the sensitivity of our results to changes in parameters. We vary each parameter independently across its assumed range (see Sec. S4.2) and look at how this affects the maximal ICU occupancy observed in the first (winter) and second (spring) waves. We choose a moderate scenario (Scenario 3) for the analysis and look at how the two peaks of ICU occupancy (one in winter, one after lifting restrictions) change in magnitude.

S4.1 Sensitivity to additional parameters

For a more precise analysis we introduce new parameters to our model (Tab S7). Firstly, we consider the possibility of previously immunised individuals having a reduced viral load and thus being less infectious. This has been reported for vaccinated individuals e.g. in Harris et al. (2021) for the Alpha variant of SARS-CoV-2, but is unclear for current and future variants. In the model, it can be represented by a change in I^{eff}, introducing a parameter σ for reduced viral load in the infectious compartments I^n and I^v:

$$I_i^{\text{eff}} = (I_i + \sigma(I_i^n + I_i^v) + \Psi M_i) \tag{45}$$

Next, we include the possibility that post-infection and vaccine-induced immunity wane at different rates Ω_n and Ω_v, respectively. Lastly, we introduce a parameter that affects the shape of $k_{\text{seasonality}}$. The transmission of SARS-CoV-2 is strongly reduced in outdoor encounters in comparison to indoor encounters. Thus, winter typically offers more opportunities for viral spread than summer because more activities are performed inside. However, the transition between summer and winter might look different than the standard sinusoidal suggested in Eq. 7. In particular, it could be the case that above a certain temperature most activities move outside all at once, resulting in a steeper transition between summer and winter as soon as temperatures allow for it. To model this, we introduce an exponent $\xi \in [0, 1]$ that modifies the sinusoidal:

$$k_{\text{seasonality}} = 1 + \mu \cdot \text{sgn}\left(\cos\left(t^\star\right)\right) \cdot \left|\cos\left(t^\star\right)\right|^\xi \quad \text{with} \quad t^\star = 2\pi \frac{t + d_0 - d_\mu}{360}\,. \tag{46}$$

That way, for $\xi \to 0$ the cosine in $k_{\text{seasonality}}$ becomes a step function.

S4.2 Parameter ranges

The way we vary parameters differs between age-dependent and non-age-dependent parameters as well as between parameters bound to the $[0, 1]$ interval (e.g., κ) and those belonging to arbitrary intervals. For the age-independent parameters $\kappa, \sigma, \xi \in [0, 1]$ we vary them in the range $[0.5, 1]$ (for κ and σ) and $[0, 1]$ (for ξ). For the age-dependent rates with arbitrary range, δ_i, $\gamma_{\text{ICU},i}$, θ_i, and $\theta_{\text{ICU},i}$, we consider a range around their default value by a factor of two. For example, for δ_i we vary across the ranges $[\frac{\delta_i^{\text{default}}}{2}, 2\delta_i^{\text{default}}]\,\forall i$ at the same time for all age-groups. Figure S7 summarises these results.

Parameters related to the memory kernel p_R, b_R, p_{vac}, and b_{vac} as well as the sensitivities to vaccine uptake α_u and α_w are also varied around their default value by a factor of two.

For age-dependent parameters related to vaccine uptake $u_i^{\text{base}}, w_i^{\text{base}}, \chi_{u_i}$, and χ_{w_i} which are bound to the interval $[0, 1]$, we look at their base value multiplied by a factor in the range $[0.8, 1.2]$ and vary one parameter for all age groups at the same time. Figure S8 summarises these results. Parameters τ_u, τ_w, t_u, t_w, $H_{\max}$, and the influx Ψ are varied in a range chosen broad enough such that an effect is observable.

The average immunity waning times $(\Omega^n)^{-1}$ and $(\Omega^v)^{-1}$ are varied in the range between 4 months and 1 year and the waning rates thus is the range of the inverse values.

S4.3 High impact parameters

In this section we discuss parameters that have a large impact on the quantitative results when being varied.

As expected, the waning rate of vaccine-induced immunity Ω^v, leads to much higher waves when increased. The peak of the wave after lifting restrictions is more than doubled for an average waning time of 4.5 months instead of the 7.5 months used as default.

The vaccine efficacy κ also plays an important role in the second wave, as by that time, most infections will originate from the waned compartments.

Naturally, the transition rates to ICU δ_i have a large impact on the magnitude of the waves. Interestingly, the impact is a lot stronger for the second wave than for the first wave. The reason is that the first wave mainly affects the unvaccinated younger age groups that are less likely to transition to ICU, whereas the second wave affects all age groups similarly.

One of the main uncertainties in our model is the choice of the sensitivity parameters α_u and α_w that modulate vaccine uptake in dependence of risk perception H_u and H_w. Lower values imply a population less reactive to threat, which results in higher waves as can be seen in Fig. S8. On the other hand, for large values of α_u and α_w, ICU occupancy seems to plateau, not decreasing any further. This suggests a limitation on what voluntary vaccination alone can do to prevent bringing ICUs to capacity limits (given our model assumptions).

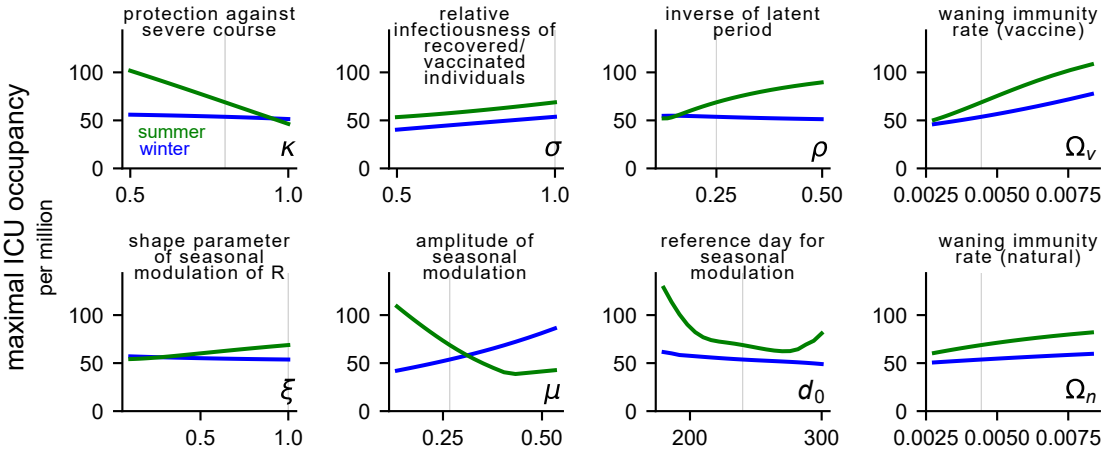

Supplementary Figure S6: **Propagation of parameter uncertainties.** Parameters are varied independently across their assumed range. The measured quantity is the maximum ICU occupancy observed in the first wave (blue) and the second wave (green). A vertical line indicates the default value of the parameter. Thus, the points where the green and blue curve intersect the vertical line have the same y-coordinate in all plots.

S5 AGE-STRATIFIED RESULTS

Figures S10-S14 show the age-stratified results for all scenarios of the main text.

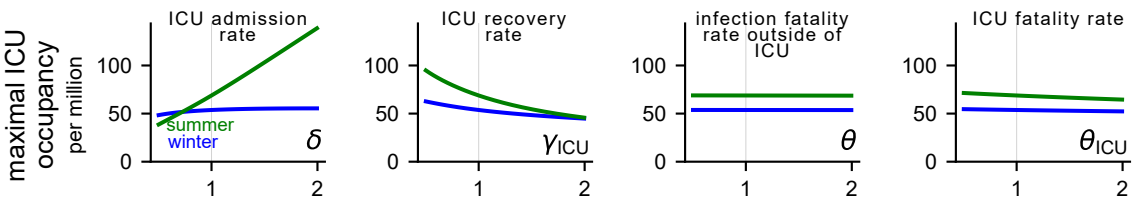

Supplementary Figure S7: **Propagation of parameter uncertainties related to age-dependent transition rates.** Parameters are varied independently across their assumed range. Note that the parameters are age-dependent (vector like) and the x-axis indicates a multiplicative factor applied to all values of the vector at the same time, instead of a single averaged parameter value. Therefore, the default parameter value indicated by the grey vertical line is always at 1.

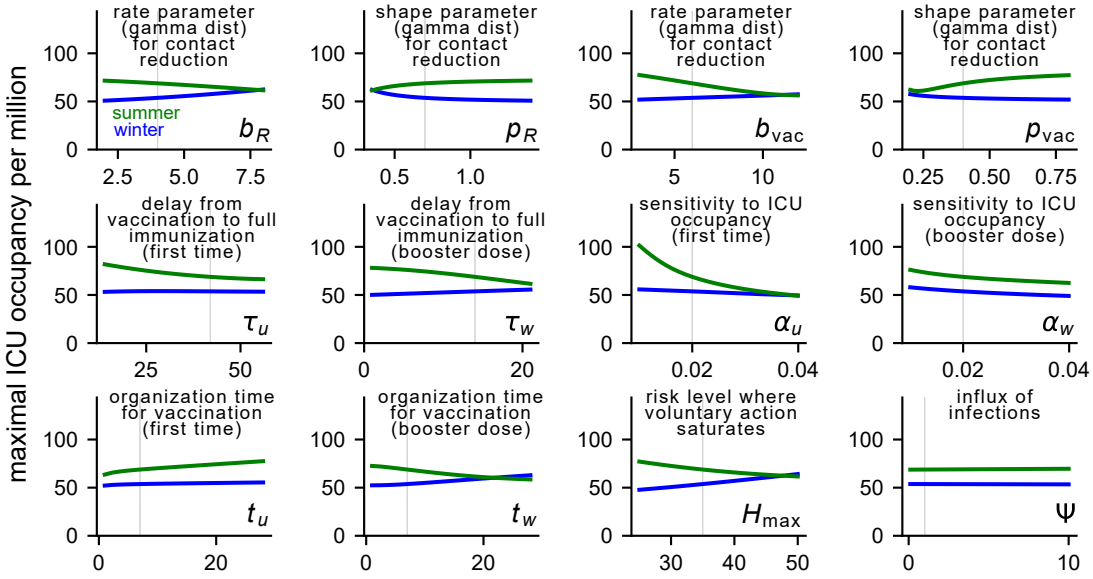

Supplementary Figure S8: **Propagation of vaccine uptake- related parameter uncertainties.** Parameters are varied independently across their assumed range. The measured quantity is the maximum ICU occupancy observed in the first wave (blue) and the second wave (green). A vertical line indicates the default value of the parameter. Thus, the points where the green and blue curve intersect the vertical line have the same y-coordinate in all plots.

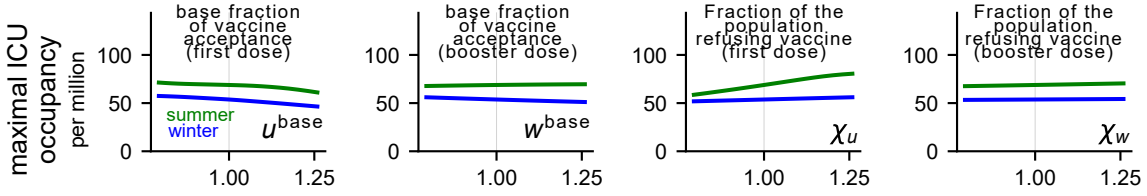

Supplementary Figure S9: **Uncertainty propagation of age-dependent parameters related to vaccine uptake.** Parameters are varied independently across their assumed range. Note that the parameters are age-dependent (vector like) and the x-axis indicates a multiplicative factor applied to all values of the vector at the same time, instead of a single averaged parameter value. Therefore, the default parameter value indicated by the grey vertical line is always at 1.

Table S5. Model variables.

Variable	Meaning	Unit	Explanation
M	Population size	people	Default value: 1,000,000
S	Susceptible compartment	people	Non-infected people, who may acquire the virus.
V	Vaccinated compartment	people	Non-infected, vaccinated people. Less likely to be infected or develop severe symptoms
W^n	Waned post-infection immunity compartment	people	Non-infected people whose post-infection immunity has already waned, thus may acquire the virus.
W^v	Waned vaccine immunity compartment	people	Non-infected people whose vaccine-induced immunity has already waned, thus may acquire the virus.
E	Nonvaccinated exposed compartment	people	Nonvaccinated, non-previously-infected people exposed to the virus.
E^n	Nonvaccinated, waned exposed compartment	people	Nonvaccinated, previously-infected people exposed to the virus whose post-infection immunity has waned.
E^v	Vaccinated exposed compartment	people	Exposed people with waned vaccine immunity.
I	Infectious compartment	people	Infectious people from the susceptible compartment S.
I^n	Nonvaccinated, waned infectious compartment	people	Infectious people from E^n.
I^v	Vaccinated infectious compartment	people	Infectious people with waned vaccine-induced immunity.
ICU	Nonvaccinated hospitalised	people	Nonvaccinated hospitalised people (from I and I^n) .
ICU^v	Vaccinated hospitalised	people	Previously-vaccinated, hospitalised people (from I^v) .
R	Unvaccinated Recovered	people	Unvaccinated recovered people (with or without requiring intensive care).
R^v	Vaccinated Recovered	people	Vaccinated recovered people (with or without requiring intensive care).
H_*	Avg. ICU occupancy	people	Auxiliary variable measuring the memory on past ICU occupancy.
$u^{\text{current}}, w^{\text{current}}$	Vaccinated individuals, independent of the compartment	–	Integral over the vaccination rates ϕ, φ.
$k_{\text{seasonality}}$	Seasonal variation of SARS-CoV-2 transmission	–	Eq. 7.
$k_{\text{NPI,self}}$	Reduction of infections due to mandatory NPIs and voluntary behaviour	–	Sec. S1.3
$\phi(t), \varphi(t)$	Administration rate of first-time and booster vaccine doses (resp.)	doses/day	Eq. 11, 13

Table S6. Initial conditions by age group. The total population size in the model is $M = 10^6$. The column $\frac{V_i^{\text{tot}}+R_i^{\text{tot}}-R_i^v}{M_i}$ shows the effective fraction of the population that is immune, which for the entire population is 68% (with $\sum_i R_i^{\text{tot}}/M = 0.2$ and $\sum_i V_i^{\text{tot}}/M = 0.6$). Sources: 1: Bauer et al. (2021), 2: Ritchie et al. (2021), 3:am RKI (2020)

ID	age group	M_i/M	$\frac{V_i^{\text{tot}}}{M_i}$	$\frac{R_i^{\text{tot}}}{M_i}$	N_i	$\text{ICU}_i^{\text{tot}}$	$\frac{W_i^v}{V_i+R_i^v}$	$\frac{W_i^n}{R_i}$	$\frac{V_i^{\text{tot}}+R_i^{\text{tot}}-R_i^v}{M_i}$
1	0-19	0.18	0.15	0.2	18.5	0.14	5%	50%	0.32
2	20-39	0.25	0.56	0.2	16.8	1.24	5%	50%	0.65
3	40-59	0.28	0.67	0.2	15.9	4.90	10%	50%	0.74
4	60-69	0.13	0.77	0.2	6.4	3.10	20%	50%	0.82
5	70-79	0.09	0.88	0.2	3.5	2.46	30%	50%	0.90
6	80+	0.07	0.95	0.2	2.3	1.62	40%	50%	0.96
Source	-	1	assumed	assumed	2	3	assumed	assumed	calculated

Table S7. Additional model parameters introduced in the sensitivity analysis.

Parameter	Meaning	Value (default)	Unit	Source
σ	Relative viral load of recovered/vaccinated individuals	1	–	Levine-Tiefenbrun et al. (2021)
Ω_n	Waning rate of post-infection immunity	$\frac{1}{125}$	day^{-1}	Tartof et al. (2021)
Ω_v	Waning rate of vaccine immunity	$\frac{1}{125}$	day^{-1}	Tartof et al. (2021)
ξ	Shape of the seasonality function $k_{\text{seasonality}}$	1	–	Gavenčiak et al. (2021)

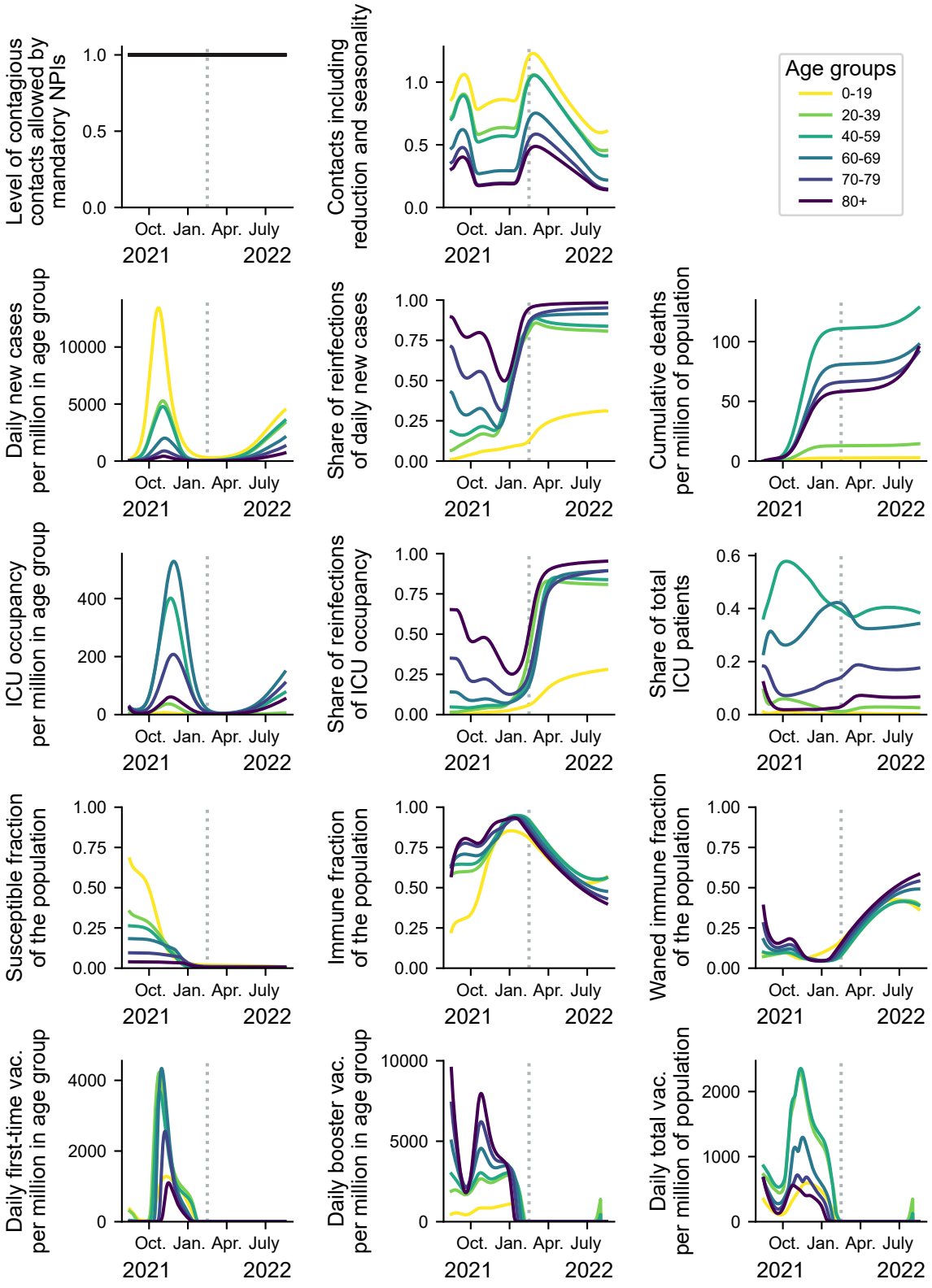

Supplementary Figure S10: **Age-stratified results for scenario 1.**

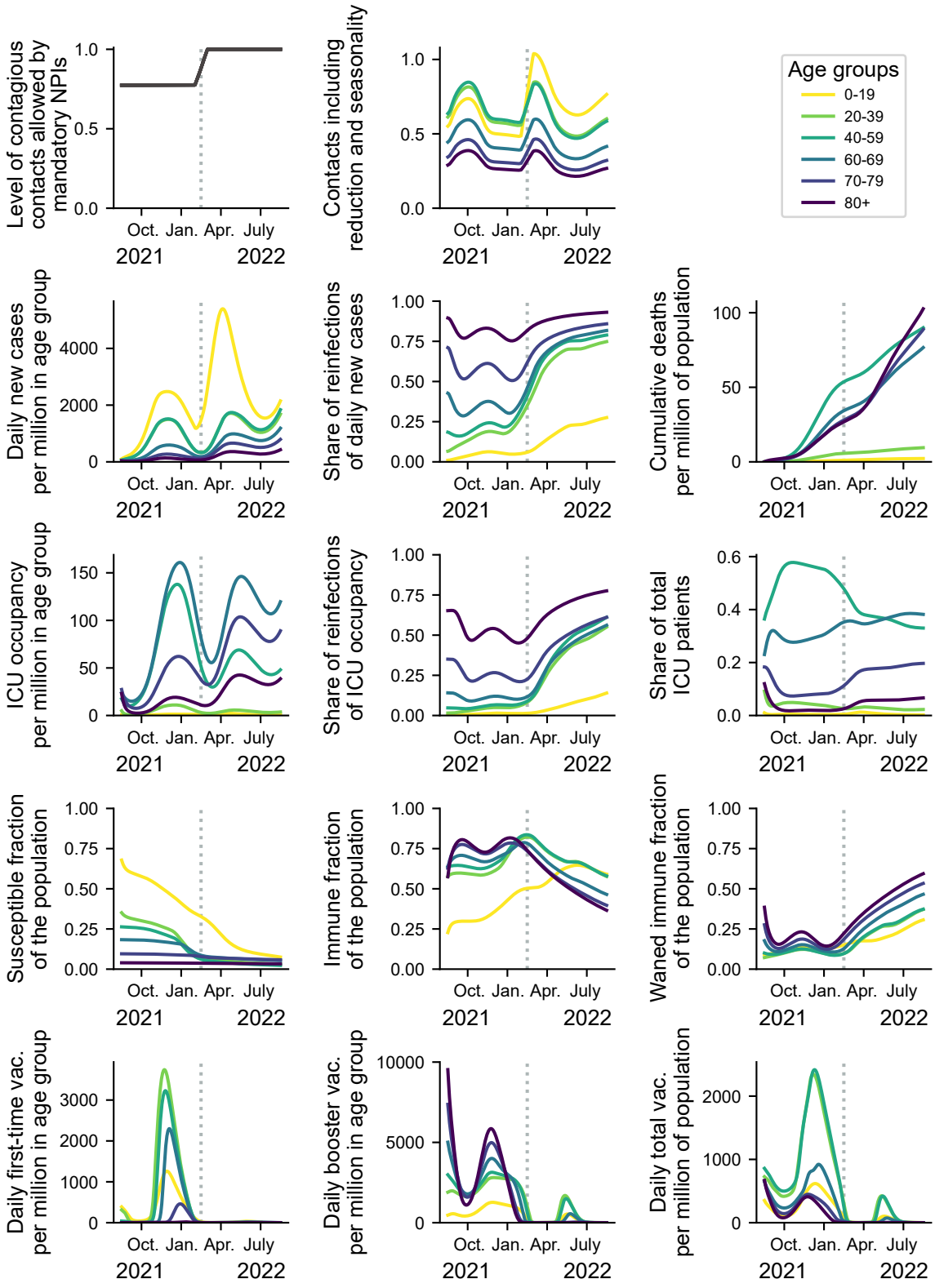

Supplementary Figure S11: **Age-stratified results for scenario 2.**

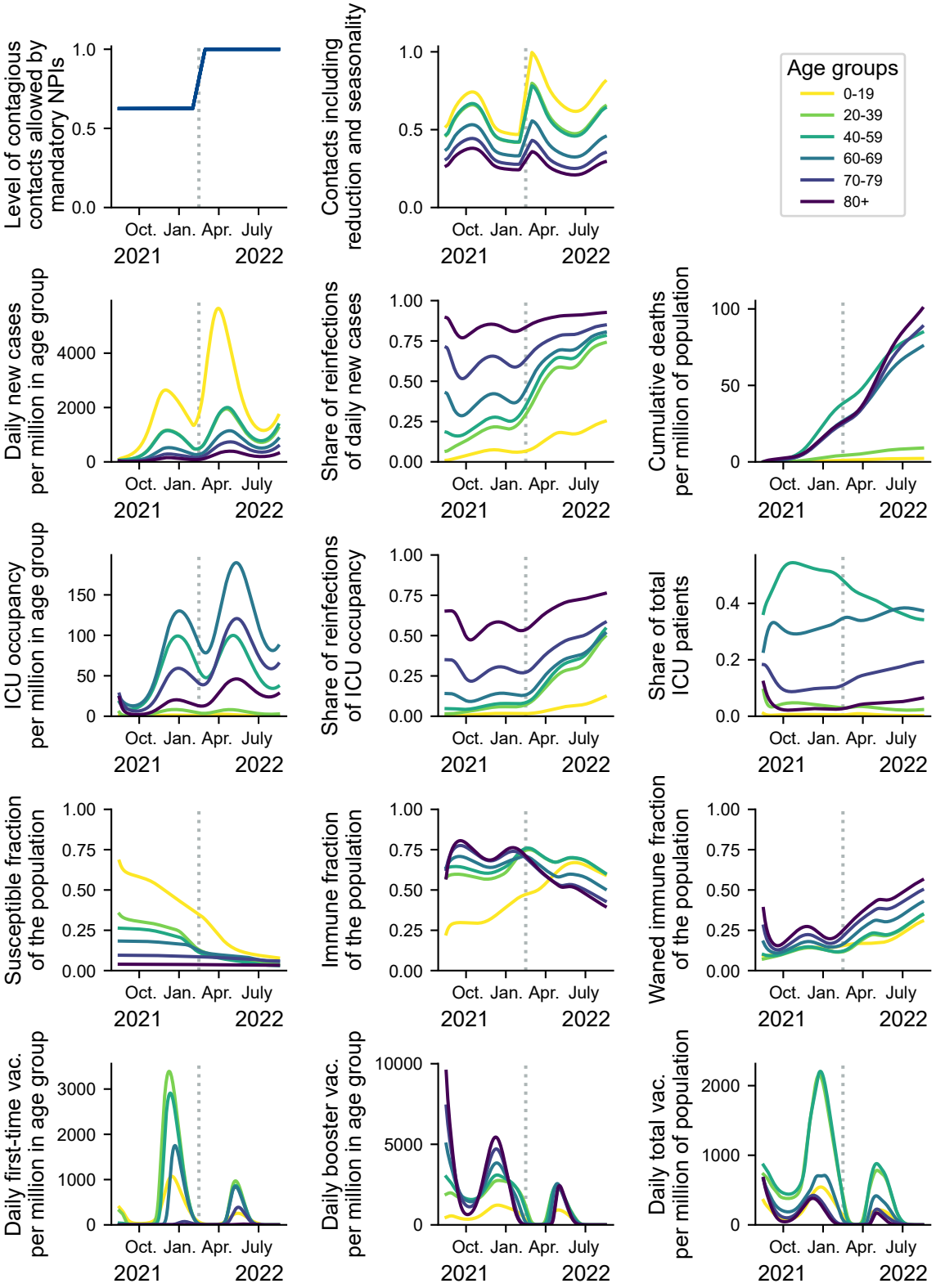

Supplementary Figure S12: **Age-stratified results for scenario 3.**

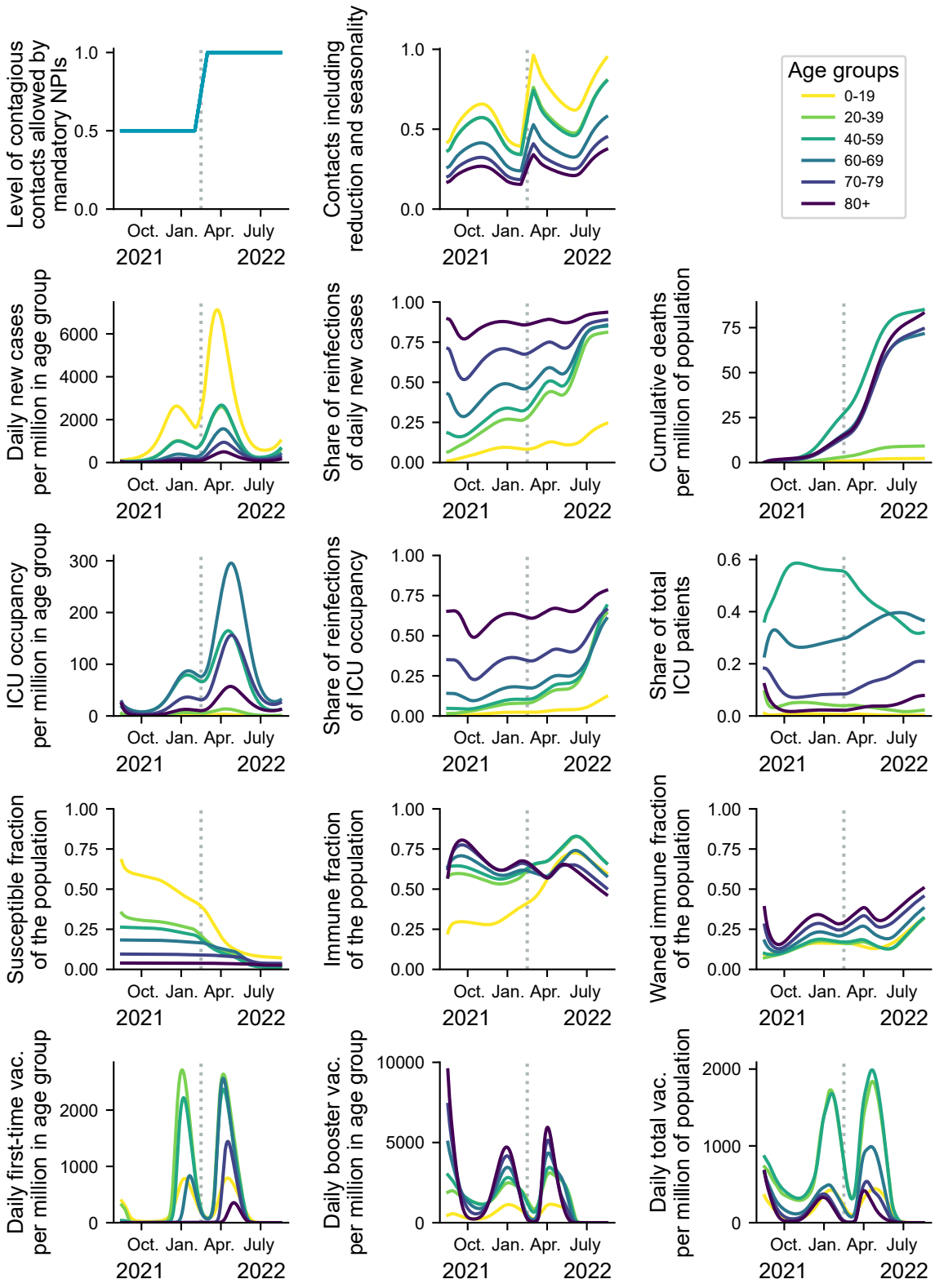

Supplementary Figure S13: **Age-stratified results for scenario 4.**

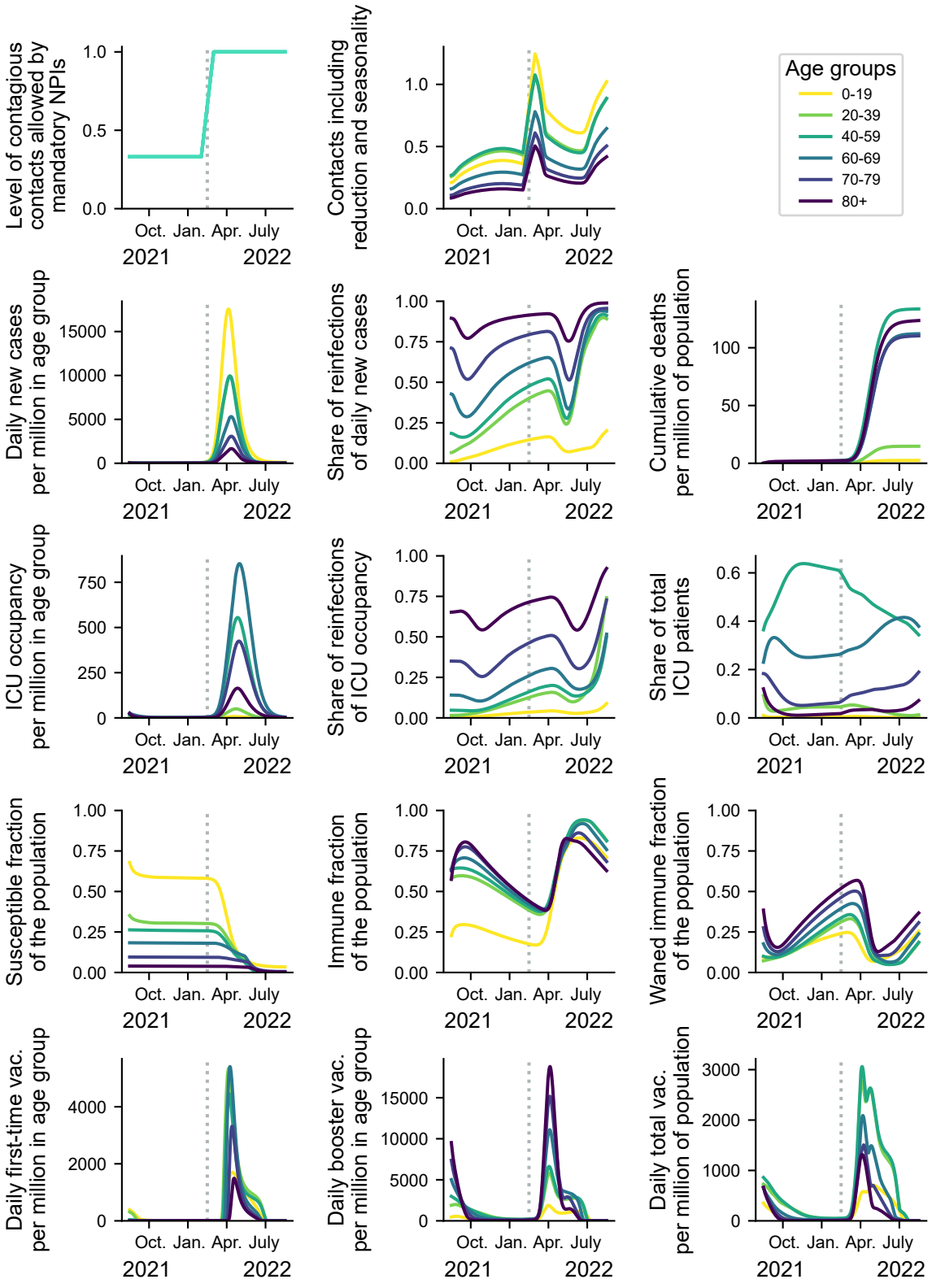

Supplementary Figure S14: **Age-stratified results for scenario 5.**

REFERENCES

Zauberman G, Kim BK, Malkoc SA, Bettman JR. Discounting time and time discounting: Subjective time perception and intertemporal preferences. *Journal of Marketing Research* **46** (2009) 543–556.

Mistry D, Litvinova M, y Piontti AP, Chinazzi M, Fumanelli L, Gomes MF, et al. Inferring high-resolution human mixing patterns for disease modeling. *Nature communications* **12** (2021) 1–12.

Diekmann O, Heesterbeek J, Roberts MG. The construction of next-generation matrices for compartmental epidemic models. *Journal of the Royal Society Interface* **7** (2010) 873–885.

Gavenčiak T, Monrad JT, Leech G, Sharma M, Mindermann S, Brauner JM, et al. Seasonal variation in sars-cov-2 transmission in temperate climates. *medRxiv* (2021). doi:10.1101/2021.06.10.21258647.

Thomas SJ, Moreira Jr ED, Kitchin N, Absalon J, Gurtman A, Lockhart S, et al. Safety and efficacy of the bnt162b2 mrna covid-19 vaccine through 6 months. *New England Journal of Medicine* (2021).

Puranik A, Lenehan PJ, O'Horo JC, Niesen MJ, Virk A, Swift MD, et al. Durability analysis of the highly effective bnt162b2 vaccine against covid-19. *medRxiv* (2021).

Turner JS, Kim W, Kalaidina E, Goss CW, Rauseo AM, Schmitz AJ, et al. Sars-cov-2 infection induces long-lived bone marrow plasma cells in humans. *Nature* (2021) 1–5.

Tartof SY, Slezak JM, Fischer H, Hong V, Ackerson BK, Ranasinghe ON, et al. Effectiveness of mrna bnt162b2 covid-19 vaccine up to 6 months in a large integrated health system in the usa: a retrospective cohort study. *The Lancet* **398** (2021) 1407–1416.

Chemaitelly H, Tang P, Hasan MR, AlMukdad S, Yassine HM, Benslimane FM, et al. Waning of bnt162b2 vaccine protection against sars-cov-2 infection in qatar. *New England Journal of Medicine* (2021).

Pegu A, O'Connell SE, Schmidt SD, O'Dell S, Talana CA, Lai L, et al. Durability of mrna-1273 vaccine–induced antibodies against sars-cov-2 variants. *Science* **373** (2021) 1372–1377.

Naaber P, Tserel L, Kangro K, Sepp E, Jürjenson V, Adamson A, et al. Dynamics of antibody response to bnt162b2 vaccine after six months: a longitudinal prospective study. *The Lancet Regional Health-Europe* **10** (2021) 100208.

Ritchie H, Mathieu E, Rodés-Guirao L, Appel C, Giattino C, Ortiz-Ospina E, et al. Coronavirus pandemic (covid-19). *Our World in Data* (2021). Https://ourworldindata.org/coronavirus.

Bauer S, Contreras S, Dehning J, Linden M, Iftekhar E, Mohr SB, et al. Relaxing restrictions at the pace of vaccination increases freedom and guards against further covid-19 waves. *PLoS computational biology* **17** (2021) e1009288.

Levin AT, Hanage WP, Owusu-Boaitey N, Cochran KB, Walsh SP, Meyerowitz-Katz G. Assessing the age specificity of infection fatality rates for COVID-19: systematic review, meta-analysis, and public policy implications. *European Journal of Epidemiology* (2020). doi:10.1007/s10654-020-00698-1.

Salje H, Kiem CT, Lefrancq N, Courtejoie N, Bosetti P, Paireau J, et al. Estimating the burden of SARS-CoV-2 in France. *Science* **369** (2020) 208–211.

Linden M, Mohr SB, Dehning J, Mohring J, Meyer-Hermann M, Pigeot I, et al. Case numbers beyond contact tracing capacity are endangering the containment of COVID-19 . *Dtsch Arztebl International* **117** (2020) 790–791. doi:10.3238/arztebl.2020.0790.

He X, Lau EHY, Wu P, Deng X, Wang J, Hao X, et al. Temporal dynamics in viral shedding and transmissibility of COVID-19 . *Nature Medicine* (2020) 1–4.

Pan F, Ye T, Sun P, Gui S, Liang B, Li L, et al. Time course of lung changes on chest CT during recovery from 2019 novel coronavirus (COVID-19) pneumonia. *Radiology* (2020) 200370.

Liu Y, Rocklöv J. The reproductive number of the delta variant of sars-cov-2 is far higher compared to the ancestral sars-cov-2 virus. *Journal of travel medicine* (2021).

Bar-On YM, Flamholz A, Phillips R, Milo R. Science forum: SARS-CoV-2 (COVID-19) by the numbers. *Elife* **9** (2020) e57309.

Li R, Pei S, Chen B, Song Y, Zhang T, Yang W, et al. Substantial undocumented infection facilitates the rapid dissemination of novel coronavirus (SARS-CoV-2). *Science* **368** (2020) 489–493.

Wouters OJ, Shadlen KC, Salcher-Konrad M, Pollard AJ, Larson HJ, Teerawattananon Y, et al. Challenges in ensuring global access to COVID-19 vaccines: production, affordability, allocation, and deployment. *The Lancet* (2021).

Betsch C, Wieler LH, Habersaat K. Monitoring behavioural insights related to covid-19. *The Lancet* **395** (2020) 1255–1256.

[Dataset] am RKI IT. Tagesreport aus dem DIVI-Intensivregister. `https://doi.org/10.25646/7625` (2020). doi:10.25646/7625.

Levine-Tiefenbrun M, Yelin I, Alapi H, Katz R, Herzel E, Kuint J, et al. Viral loads of delta-variant sars-cov-2 breakthrough infections after vaccination and booster with bnt162b2. *Nature Medicine* (2021) 1–3.

Harris RJ, Hall JA, Zaidi A, Andrews NJ, Dunbar JK, Dabrera G. Impact of vaccination on household transmission of sars-cov-2 in england. *medRxiv* (2021).